Available online at www.sciencedirect.com
SCIENCE DIRECT
Journal of Sound and Vibration 296 (2006) 334–352
JOURNAL OF SOUND AND VIBRATION
www.elsevier.com/locate/jsvi

Characterisation of an airborne sound source for use in a virtual acoustic prototype

A.T. Moorhouse[a,*], G. Seiffert[b]

[a]Acoustics Research Centre, University of Salford, Manchester, UK
[b]Acoustics Research Unit, University of Liverpool, Liverpool, UK

Received 11 March 2005; received in revised form 3 March 2006; accepted 6 March 2006
Available online 26 May 2006

Abstract

An approach is outlined suitable for constructing 'virtual acoustic prototypes' of machines. Here, the machine is 'sub-structured' into: active components (vibro-acoustic sources), and frame (the remaining passive parts of the machine). The approach is validated using the illustrative example of an electric motor installed in a machine frame. The motor is characterised by a line of four monopoles on its axis, the complex source strengths for which are obtained from the measured anechoic sound field around the motor using an inverse method. A singular value decomposition is carried out both to aid the solution and to shed light on the dominant mechanisms. A set of compatible transfer functions of a machine frame is then measured using a reciprocal technique. The sound power of the assembled machine is then predicted using a 'virtual prototype' approach of combining motor and frame data in the computer. Reasonable agreement is obtained with measurements made on a real prototype, although the agreement was limited at least in part by difficulties in repeating the same operating conditions for the motor. A simplified characterisation, using a single monopole, and with improved motor control produced excellent agreement.

1. Introduction

The overall context for this paper is the increasing need for quieter and more pleasant sounding machines and equipment in the home, workplace and the environment. In order to meet this demand, manufacturers need to find faster and cheaper alternatives for acoustic testing than traditional physical prototypes. The automotive sector, which has moved increasingly towards virtual acoustic prototypes for noise evaluation over recent years, illustrates the potential advantages of the virtual approach. In this paper an approach to virtual acoustic prototyping is described, which is more adapted to medium technology industries, like white goods, domestic and outdoor products, etc. who do not have the resources or expertise to develop large-scale numerical models, but who nevertheless need a systematic approach to acoustic design. The approach was developed during the recently completed EC Framework V sponsored project Nabucco.

*Corresponding author. Tel.: +44 161 295 5490; fax: +44 161 295 4442.
E-mail address: a.t.moorhouse@salford.ac.uk (A.T. Moorhouse).

0022-460X/$ - see front matter © 2006 Elsevier Ltd. All rights reserved.
doi:10.1016/j.jsv.2006.03.017

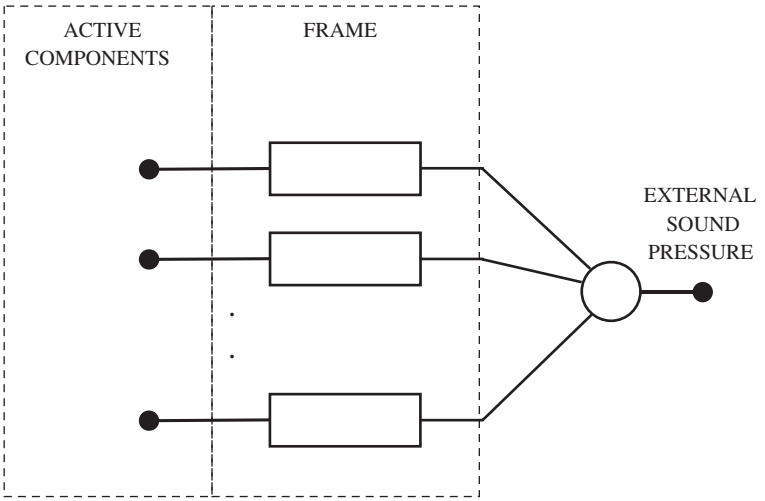

Fig. 1. Schematic of overall prediction scheme.

In the approach (known as Noise Shaping Technology or NST) a machine is divided into substructures in two classes (Fig. 1):

- active 'components',
- the remaining passive parts of the machine (comprising panels, air cavities, pipes, etc.), which will be referred to collectively as the 'frame'.

The complete working machine consists of the assembly of the 'active components' and 'frame'. The machine frame is purely passive, and does not generate noise itself, but receives and transmits vibro-acoustic excitation by the source components. In doing so the frame imposes its character on the noise emitted by the component and the overall output from the assembled machine therefore depends on both component and frame.

One of the most common comparisons a designer needs to make is to compare 'active components' (like motors, pumps, fans and compressors), which can only be achieved when they are installed in the intended machine or equipment. Comparing the characteristics of the active components alone (such as sound power), without including the effect of the frame or other components of excitation such as structure-borne excitation can (and often does) lead to an incorrect rank ordering. Thus, a prototype of the assembled machine is required in order to properly compare active components. The background to this work is the appeal of constructing the necessary prototypes in a virtual sense, for example using the above-described NST approach.

The objective of the work presented here is to validate the above approach through the example of an electric motor installed in a machine frame. The target quantity for validation is the sound power of the assembly. This requires the motor to be characterised independently of the frame, and the frame to be characterised using a compatible set of transfer functions. Only airborne excitation is considered in this paper; a parallel procedure carried out for structure-borne excitation by the motor is considered briefly in Refs. [1,2] and will be detailed in a later paper. The approach is based on measured data, and whilst this implies that the structures, or similar ones, must exist, the approach can properly claim to be a virtual approach since it allows *assemblies* of components and frames to be studied that do not physically exist.

2. Overview of prediction scheme

As described above, the overall noise output of the machine is considered a combination of component characteristics, and frame characteristics. Mathematically this can be expressed as

$$\mathbf{p} = \mathbf{H}\mathbf{q}, \tag{1}$$

where **p** is the vector of predicted sound pressure at any desired position, **q** is a vector of source strengths, and **H** is the transfer function matrix relating sound pressure output to source strength input and quantifies the transmission through the machine frame.

Effective use of Eq. (1) hinges largely on how to represent the source strength **q**, specifically on how to represent the spatially continuous excitation by the source as a finite number of parameters to populate the vector **q**. The approach here is to replace the real source with an 'equivalent source system' made up of a number of elementary sources. This is not a new idea, the same general approach was suggested by Cremer [3] and has also appeared in the literature under various guises: the 'source simulation technique' [4], the 'method of auxiliary sources' [5], the 'wave superposition' method [6], the 'method of equivalent sources' [7], 'equivalent sphere method' [8] and probably others. The approach is often used in conjunction with numerical methods to predict radiation from vibrating bodies of arbitrary shape, for example as an alternative to boundary element methods (for example see Refs. [4,6]). There are also examples of the approach being used in conjunction with measured transfer functions [9,10] as will be done here. Various choices of elementary sources are possible, such as multipoles [11], combinations of monopoles and dipoles [12], and spherical functions [8,13] (these are just some examples of numerous possible references).

The equivalent source system adopted for this study is a line of monopoles on the motor axis as shown in Fig. 2. A similar scheme was investigated in Ref. [14]. The elements of **q** are the complex volume velocities. Any number of monopoles could be selected, but four was chosen as a compromise between what was practical, and what was likely to give a sufficiently detailed representation of axial directivity patterns of the motor. The axial monopoles of course do not model angular directivity patterns, but this was felt to be unnecessary after preliminary measurements showed there to be no strong angular dependence of sound pressure level around the motor. (A little care is needed here since the sound pressure levels are time-averaged and do not distinguish between, for example, symmetric and antisymmetric source mechanisms. Nevertheless, the axisymmetric assumption was considered reasonable.) A practical advantage of representing the source by several conveniently spaced monopoles is that transfer functions can be measured reciprocally with a microphone at the position of each fictitious source (as will be described later). If the positions are sufficiently close then such an arrangement can also be considered to approximate a multipole.

It should be noted that the requirement in this approach is to 'characterise' the source as distinct from 'modelling' it. In the former the aim is not necessarily to obtain an accurate representation of source mechanisms, but rather to represent their net effect on the surroundings. For the current purposes the target is

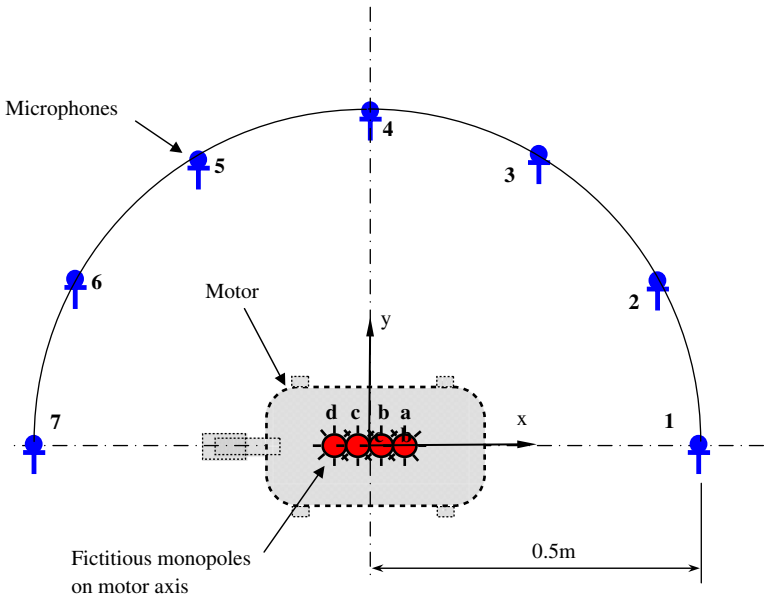

Fig. 2. Motor showing positions of monopoles forming equivalent source, and microphone positions for free field measurements.

to predict the sound power from an assembly of component and frame. Therefore, the source characterisation only needs to include a concomitant level of detail.

Having decided on the form of the equivalent source system an experimental technique is required to obtain the strengths of the equivalent sources. Possible methods include direct measurement of surface velocity, use of intensity methods to infer the equivalent volume velocity of fictitious surface monopoles [9,10], as well as a range of inverse techniques, most notably acoustic holography [15]. In Refs. [9,10] the radiation of sound was entirely due to vibration of surfaces. However, sound radiation from the motor under study here is due to a combination of vibration and aerodynamic sources. Therefore, an approach based on measurement of the surface velocity would not be successful and there is little alternative but to measure the radiated field and back-calculate the source strengths by inverse methods.

An important requirement of the source characterisation is that $\mathbf{q}$ and $\mathbf{H}$ are independent properties of the source and frame, respectively. If this condition is not met then the source data will not be transferable to other frames, nor the frame data to other sources. Thus, the equivalent source system must be selected such that $\mathbf{q}$ is independent of the surroundings. This condition is met if the surrounding air does not load the source so as to alter the sound generating mechanisms. It is reasonable to assume that the cavity impedance does not affect vibration of the motor casing, but there is also some aerodynamic sound generation around the rotor. Aerodynamic sources are potentially affected by cavity impedance as acknowledged in two port methods for fan characterisation, as exemplified in Ref. [16]. However, it is assumed that the immediate environment around the rotor is associated more with the geometry of the motor casing than that of the machine frame and that it is unlikely that the source mechanisms will vary from one frame to another.

As well as the potential loading effect of the cavity impedance on the source mechanisms as just described, it is also necessary to consider the complementary effect, i.e. the potential effect of the source impedance on the cavity response. In particular, the equivalent source system does not account for the volume of the motor which could potentially affect cavity modes. Here, it was argued that since the volume of the motor is small relative to the cavity that the effect could be neglected. As a brief check on this assumption a simple finite element analysis confirmed that the 'missing' volume of the motor would not unduly affect cavity resonances.

The only alternative to the above assumptions would be to use a more rigorous source characterisation which also included source impedance, such as proposed by Bobrovnitskii and Pavic [17]. However, this would complicate measurements enough to make the approach unfeasible for popular use.

To summarise, it is assumed that the source is of negligible volume and has invariant volume velocity. Whilst these assumptions do imply some loss of rigour, they are considerably less restrictive than the assumption of constant sound power often used for evaluation of machinery noise. In practice, the sound power of enclosed sources can, and does, vary due to interference caused by nearby reflecting surfaces etc. The equivalent source system considered here allows such variation by including the effects of reflection in the transfer function $\mathbf{H}$. Thus, variations in source sound power due to the frame are taken into account.

One final comment of great importance for practical cases concerns the operating conditions of the motor. It is known that sound generation by electric motors, as well as many other active components, may be strongly affected by operating conditions, in particular by mechanical load. Reasonable predictions can only be obtained if the motor is characterised whilst performing under a realistic loading regime, which presents some significant measurement challenges. The emphasis in this paper is on validation, so all measurements were conducted on an unloaded motor (it was not possible to perform reliable validation measurements under load because the load itself generates noise and because structure-borne noise cannot be avoided). Measurements on a loaded motor were conducted but are reported elsewhere [18,19].

3. Characterisation of the motor as a sound source

Measurements were conducted on the source in anechoic conditions. The equation to be solved to obtain the source strengths is

$$\mathbf{p_0} = \mathbf{H_0 q}, \tag{2}$$

where the subscript $\mathbf{0}$ indicates free field and distinguishes the transfer function and sound pressure from those for the installed motor (Eq. (1)).

Calculation of equivalent source strengths involves three main steps (see Fig. 2 and Eq. (2)):

(a) measurement of free field sound pressure field around the motor, $\mathbf{p_0}$
(b) calculation of the free field transfer functions between monopoles and microphone positions, $\mathbf{H_0}$
(c) solution for unknown volume velocities $\mathbf{q}$.

3.1. Measurement of sound pressure field

The sound pressure field was measured with 7 microphones equally spaced around one side of a 0.5 m circle as shown in Fig. 2. It is assumed that the motor is an axisymmetric source. Since there are 7 microphone and 4 monopoles the system is overdetermined.

3.2. Free field transfer function matrix

The Green's function for a monopole in free space is well known and is given by

$$h_{0,RS} = -\frac{\mathrm{i}\rho ck}{4\pi}\frac{\mathrm{e}^{-\mathrm{ik}(|\mathbf{R_R}-\mathbf{R_S}|)}}{(|\mathbf{R}_R-\mathbf{R}_S|)}, \tag{3}$$

where $\mathbf{R}_R = x_R\mathbf{i} + y_R\mathbf{j} + z_R\mathbf{k}$, $\mathbf{R}_S = x_S\mathbf{i} + y_S\mathbf{j} + z_S\mathbf{k}$ are the vector co-ordinates of the source and response point respectively. The co-ordinates of the 4 monopoles and 7 microphones are given in Table 1. By substituting these co-ordinates into Eq. (3) the transfer function matrix is built up relating all four sources (S_1-S_4) to all 7 sound pressures (R_1-R_7):

$$\mathbf{H_0} = \begin{Bmatrix} h_0(R_1|S_1) & h_0(R_1|S_2) & \ldots & h_0(R_1|S_4) \\ h_0(R_2|S_1) & . & & . \\ . & & . & \\ . & & & . \\ h_0(R_7|S_1) & . & . & h_0(R_7|S_4) \end{Bmatrix},$$

where the subscript **0** indicates free field.

3.2.1. Singular value decomposition (SVD) of the free field transfer function matrix

The calculated transfer function matrix is decomposed using a SVD.

$$\mathbf{H_0} = \mathbf{U_0}.\mathbf{S_0}.\mathbf{V_0^H} \tag{4}$$

The matrix $\mathbf{V_0}$ is a 4×4 square matrix, the columns of which are vectors corresponding to certain distinct spatial patterns in the strengths of the four monopole sources. These are the 'input singular vectors' or 'input modes' (the term 'mode' here differs from the usual use of the term to describe normal modes of the system). Illustrated in Fig. 3a (lower plot) are the input modes for a frequency of 250 Hz and a source spacing of

Table 1
Coordinates of monopole and microphone positions

	1	2	3	4	5	6	7
x_R	.5	.433	.25	0	−.25	−.433	−.5
y_R	0	.25	.433	.5	.433	.25	0
z_R	0	0	0	0	0	0	0
x_S	3d/2	d/2	−d/2	−3d/2			
y_S	0	0	0	0			
z_S	0	0	0	0			

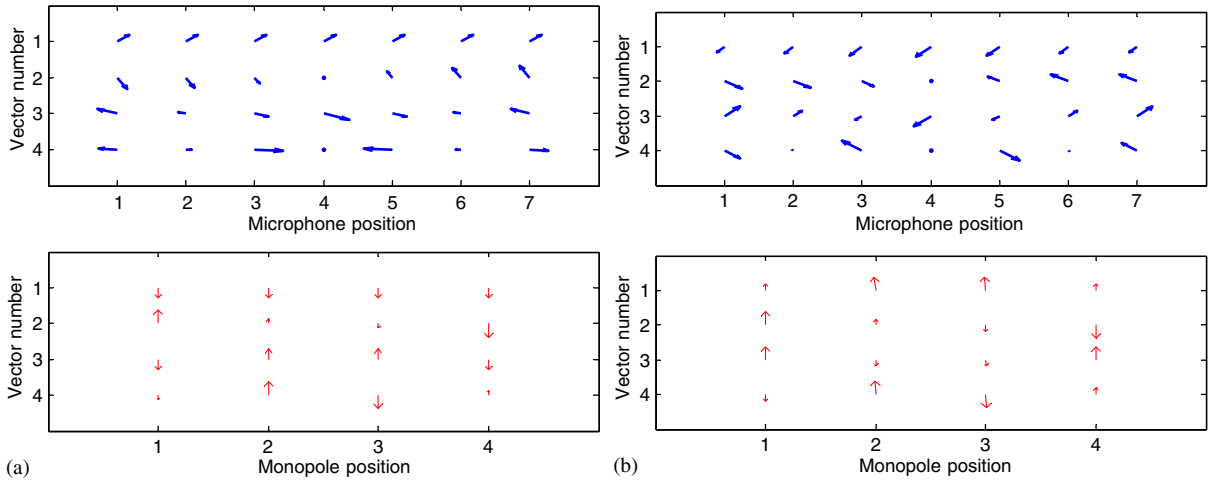

Fig. 3. Output (upper) and input (lower) singular vectors (input and output modes) from calculated free field transfer function matrix at (a) 250 Hz and (b) 5000 Hz. The length of the arrow represents the magnitude of the (dimensionless) vector element, and the angle its phase.

12 mm. In the first mode the magnitude and phase are approximately equal for all four monopoles. In this case the equivalent source acts something like a single large monopole. The second input singular vector corresponds approximately to a dipole-like pattern where the monopoles at either end are equal and opposite. The third and fourth input singular vectors correspond to more complicated higher-order patterns.

Corresponding to each input mode is an 'output singular vector' or 'output mode', that is a certain pattern of sound pressure at the 7 microphone positions. These vectors are the columns of the matrix $\mathbf{U_0}$. They are shown in Fig. 3(a) (upper plot) for a frequency of 250 Hz. In the first mode, the sound pressure at all positions is equal in magnitude and phase. In other words we have an omnidirectional pattern corresponding to the monopole type excitation of the first input mode. The second has a dipole type pattern corresponding to the second input mode. The third and fourth output modes can also be seen to emulate the shape of the corresponding input modes (compare Fig. 3(a) upper and lower plots).

As described above, the first input mode bears some resemblance to a single equivalent monopole, but the correspondence is not exact and varies with frequency. This is illustrated in Fig. 3(b) which shows the input and output modes at 5000 Hz. For the first mode all excitations are in phase, as are all responses. However, the magnitude is not equal at all positions, in other words, the sound pressure field is not omnidirectional as it would be for a single monopole at the centre of the equivalent source. For this reason, it may be more accurate to describe this as a 'zero order' excitation and response. Subsequent modes correspond to first, second and third order. This is clarified in Fig. 4 where the directivity patterns due to the four input modes are plotted at 250 and 5000 Hz. The monopole- and dipole-like patterns are clearly seen. The order of the mode is seen to correspond to the number of zeros in a half circumference of the directivity plot.

In Figs. 3(a) and (b) the shapes of the input and output modes match; in-phase symmetric patterns for the first mode (zero order), anti-symmetric patterns for the second (first order), symmetric and anti-symmetric patterns in both input and response for the third and fourth modes (second and third order) respectively. This behaviour continues up to about 5 kHz, above which the furthest monopoles are separated by more than a half wavelength. This separation of the sources does not violate any assumptions, but it means that the combination of four monopoles no longer approximates a single multipole. Thus, above 5000 Hz an input in a particular pattern can result in very different spatial pattern in the output, and the classification of the modes as zero order, etc. is less appropriate.

Each pairing of input and output modes is connected by a constant, the singular value, which form the elements of the diagonal matrix $\mathbf{S}$ in Eq. (4). The singular value can be interpreted as the magnitude of the output mode due to an excitation of unit magnitude in the corresponding input mode. Since in this case the output is a sound pressure and the input a volume velocity, the square of the singular value can be thought of

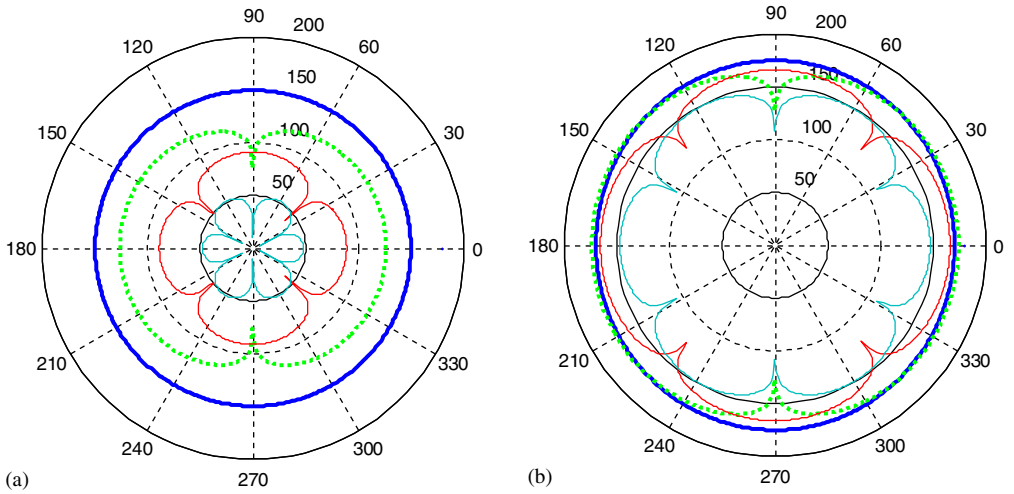

Fig. 4. Directivity patterns in free field sound pressure level (dB re 20-μPa) corresponding to the four input modes at (a) 250 Hz and (b) 5000 Hz; ___, zero order; ••••, first order; ___, second order; ...., third order.

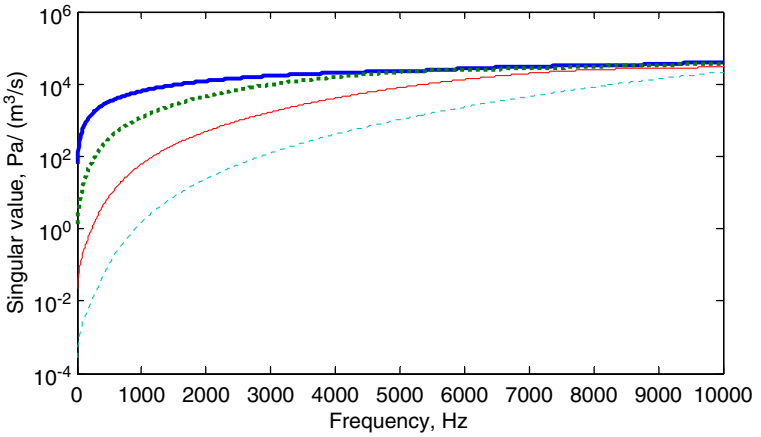

Fig. 5. Singular values from calculated free field transfer function as a function of frequency for 12 mm spacing of the monopoles.

as a kind of radiation efficiency for that spatial pattern. Thus, the first singular value relates the strength of a monopole type response to a monopole type excitation, the second a dipole type response to a dipole type input and so on for the higher-order modes.

Fig. 5 shows the singular values for 12 mm spacing. The form of the curves is reminiscent of plots of the radiation efficiencies of multipoles of increasing order, although as mentioned above, there is not an exact correspondence to a multipole due to the finite spacing of the monopoles. In-phase symmetrical patterns are significantly more efficient radiators than dipole and higher-order patterns at low frequency. At high frequencies all orders tend towards equal efficiency.

3.3. Solution for source strengths

To solve for the source strengths Eq. (2) is written in terms of the SVD of the transfer function matrix from Eq. (4)

$$\mathbf{p_0} = \mathbf{H_0 q} = \mathbf{U_0}.\mathbf{S_0}.\mathbf{V_0^H q}. \tag{5}$$

Premultiplying by $\mathbf{U_0}^{\mathrm{H}}$ and using the unitary property ($\mathbf{U_0}^{\mathrm{H}}\mathbf{U_0} = \mathrm{I}$) the equation is transformed into

$$\mathbf{r_0} = \mathbf{S_0 s} \tag{6}$$

which is of the form of an input/output system. In Eq. (6), $\mathbf{r_0} = \mathbf{U_0^H p_0}$is a 4×1 column vector each element of which is the projection of the measured sound pressure vector onto one of the output modes. $\mathbf{r_0}$ therefore quantifies the participation of each of the output modes in the overall measured sound pressure. $\mathbf{s} = \mathbf{V_0^H q}$ is a 4×1 vector, as yet unknown, which quantifies the participation of the input modes. The matrix $\mathbf{S_0}$ contains the factors relating the strengths of the input and output patterns (the singular values), and since it is diagonal and non-singular, the formal solution is simple:

$$\mathbf{s} = \mathbf{S_0^{-1} r_0}. \tag{7}$$

Fig. 6(a) illustrates the magnitude of the elements of $\mathbf{r_0}$, calculated from $\mathbf{r_0} = \mathbf{U_0^H p_0}$. The first element of $\mathbf{r_0}$ quantifies the contribution of the first output mode to the overall measured sound pressure (at each frequency), and similarly for elements two to four. Thus, the sum of the squares of the curves in Fig. 6(a) equals the sum of the squares of the measured sound pressure, $|\mathbf{r_0}|^2 = |\mathbf{p_0}|^2$. All modes are seen to be of comparable importance. Fig. 6(b) shows the participation of the input modes as calculated from Eq. (7), and Fig. 7 shows the source strengths calculated from $q = \mathbf{V_0} s$. The results in Fig. 6(b) illustrate a well-known problem of inverse methods: when the participation factors for the input modes are calculated using a straightforward inverse, the contribution of higher-order modes is greatly exaggerated by their small radiation efficiency. As a result, the highest-order mode is apparently the dominant input mode over the entire frequency range. This is almost certainly not an accurate physical description, but results from the fact that random measurement errors tend to give a false emphasis to the higher-order modes.

A possible solution to this problem is 'singular value discarding' (see for example Refs. [20–22] in which a number of the input and output modes (usually corresponding to the smallest singular values) are rejected, it being assumed that they play no part in the physical process. In the case of a measured transfer function matrix, those modes which are entirely due to noise in the measurements are rejected. In the case studied here the transfer function matrix is calculated and all modes can be assumed to be 'real', that is not entirely due to noise. Nevertheless, it has been shown in Fig. 6 that selection of the important modes is necessary to avoid amplification of errors in the measured sound pressure vector on inversion. One disadvantage with this form of regularisation is that discarding a mode is equivalent to removing energy from the system, which is undesirable, especially since the target quantity in this case is the sound power. To circumvent this problem a method of compensating for the lost energy was developed and is reported in Ref. [23].

Fig. 8(a) shows the measured sound pressure magnitude around the motor at the 500 Hz peak. Also shown are the reconstructed directivity patterns using respectively one, two, three and four modes (in which the compensation procedure [23] has been invoked. In this figure, the difference between each curve and the measured points (marked with small circles) indicates the inevitable error obtained with an overdetermined system, i.e. when the sound pressure at the seven field points is reconstructed with fewer than seven sources. The zero-order term (thick solid line) is able to reconstruct only an omni-directional pattern. With two terms

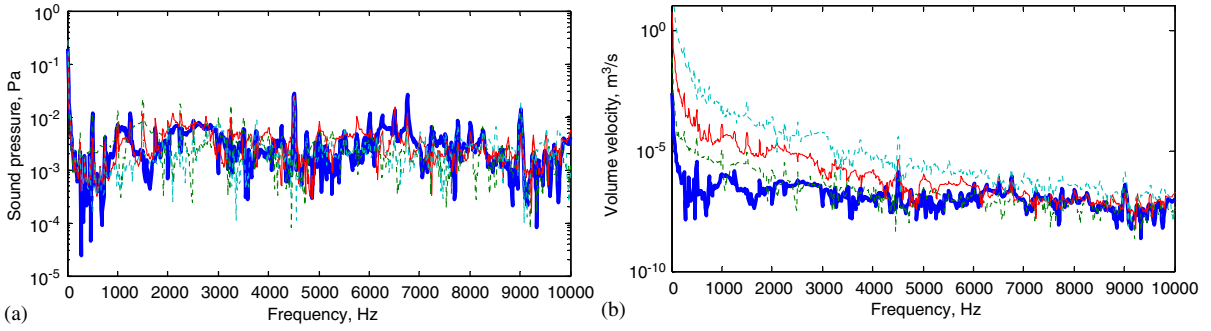

Fig. 6. Participation factors of (a) output modes, and (b) input modes as calculated from the measured sound pressure by a straightforward inverse procedure: ___, zero order; ••••, first order; ___, second order; ...., third order.

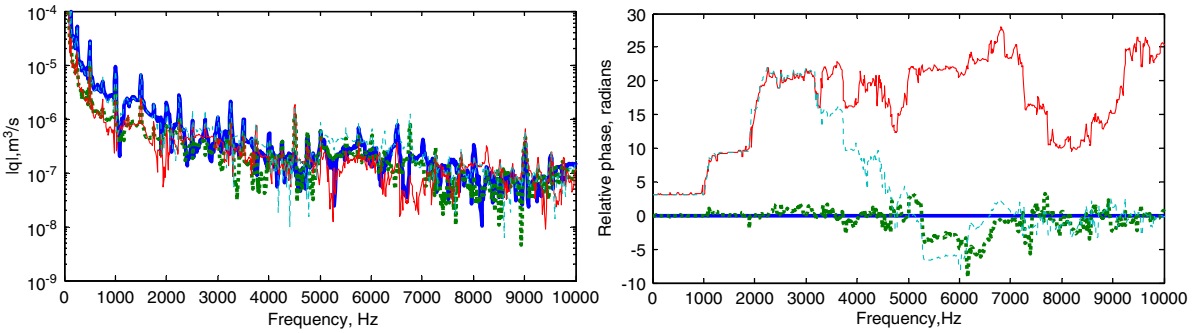

Fig. 7. Source strength of monopoles a–d, top magnitude, bottom phase.

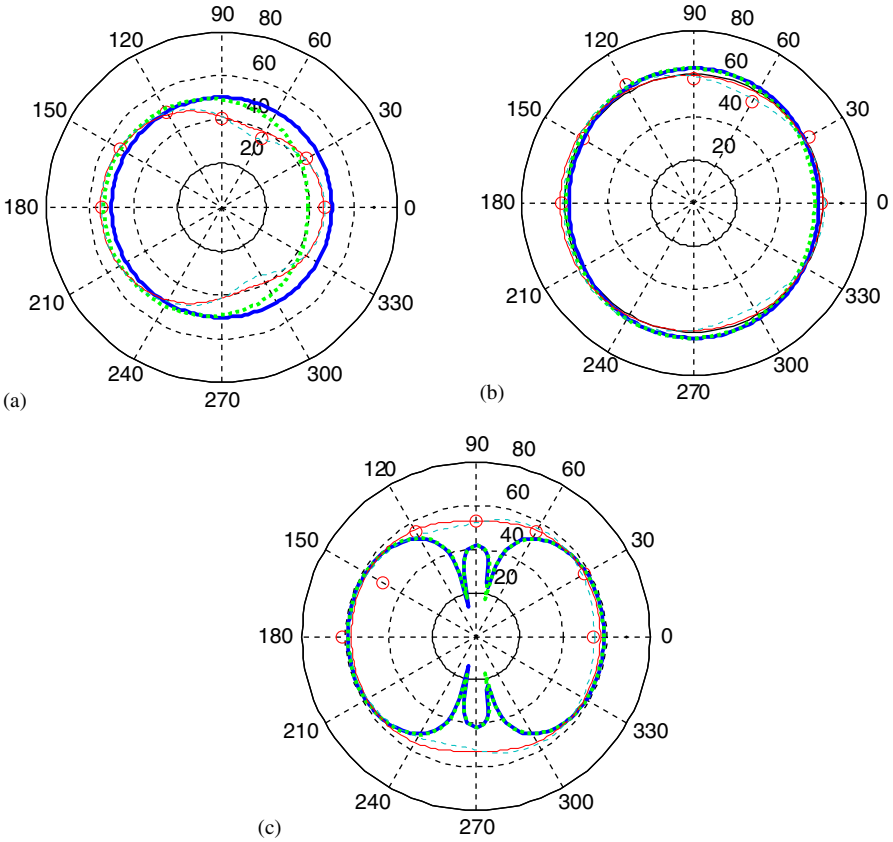

Fig. 8. Reconstructed sound pressure level (dB re 20-μPa) compared with measured sound pressure level for peaks at (a) 500 Hz, (b) 4512.5 Hz, (c) 9012.5 Hz, zero, measured values. Lines are reconstructed sound pressure using; ___, zero-order terms only; ••••, zero and first order; ___, zero, first and second order, ----, all four orders.

(thick dotted line) a directional pattern is possible, and the levels at the left end of the motor are approximately 15 dB higher than at the right end. With three and four terms retained, the measured directivity is reproduced with more and more detail. Thus, the effect of truncation is to smooth the directivity pattern of the equivalent source. However, due to the compensation procedure [23], the spatial averaged sound pressure for all curves is equal to the measured value. Thus, errors in sound power do not occur even when truncating to a single term, and the only error introduced by truncation is in the directivity. The equivalent source can then be considered 'equivalent' in the sense that its free field sound power is identical to that of the real source (within

measurement accuracy), and its directivity pattern matches as closely as is allowed by the number of terms selected.

Similar, although less pronounced trends are displayed for the 4512.5 Hz peak in Fig. 8(b). In Fig. 8(c) the patterns for the 9012.5 Hz peak are seen to display different trends. This is because the monopoles in the equivalent source are separated by more than a half wavelength for frequencies above 5000 Hz, as reported in relation to Fig. 3(b). It appears that for the higher frequencies it may be necessary to include at least three terms in order to avoid destructive interference effects shown for the first two modes.

We recall that the objective is to predict the sound power output of the installed motor. It may not be necessary to model directivity in detail unless this has an effect on the power radiated from the machine frame once the motor is installed. With this in mind the compensation procedure allows considerable flexibility in discarding singular values. However, some care should be exercised to ensure that the physical mechanisms are adequately described. For example, dipole-type patterns may not show strong directivity, but may couple with antisymmetric modes inside the machine frame. Also, Tomilina et al. have described the phenomenon of 'source order lowering' [24] which could lead to errors if the order of the source is not correctly modelled.

At this stage it is not possible to be definitive about which modes can be safely rejected. This is because the contribution of each mode to the sound power of the assembled machine depends both on its strength, and on the sensitivity of the machine frame to excitation in that particular spatial pattern. The question of frame sensitivity will be examined in the next section. In the mean time it is necessary to make some judgement, since the behaviour of the machine frame will not always be known in advance.

Bearing in mind the above comments the following selection of singular values was made:

- the zero- and first-order modes were retained at all frequencies,
- the second-order mode was rejected below 5000 Hz,
- the third-order mode was rejected at all frequencies.

4. Transfer functions of machine frame

The reception positions around the machine at which sound pressure is to be evaluated are shown in Fig. 9. These positions are selected according to ISO3744 [25]. To measure transfer functions by a conventional method would require placing a monopole source at each of the positions of the equivalent sources inside the frame (a–d) and measuring the sound pressure response at these external positions (1–6). This is impracticable due to the limited space inside the frame, and the difficulty of precisely positioning the source. As a more practical alternative, the reciprocity principle has been invoked, which by now has been well established for such measurements [26].

4.1. Reciprocal measurement of transfer functions

In the reciprocal measurements, the positions of source and receiver are interchanged so that an omnidirectional source of known volume velocity is required at each external position, and four microphones are placed inside the frame on the axis of the motor (the motor is removed). The test arrangement is illustrated schematically in Fig. 10.

The required transfer functions are the ratios of external pressure due an internal monopole. By reciprocity, this is equal to the internal pressure due to an external monopole:

$$h(R_1|S_a) = p_1/q_a = p'_a/q'_1 \tag{8}$$

where h is the element of the transfer function matrix $\mathbf{H}$, p_1, q_a are the pressure and volume velocity for the forward experiment, and p'_a/q'_1 are the internal pressure and external volume velocity in the reciprocal experiment. The prime is to distinguish a reciprocal measurement from a forward measurement, but will now be dropped for clarity. To take the measurements, the external source is moved from position 1 to 6, and at each the pressure at microphones a-d is recorded simultaneously.

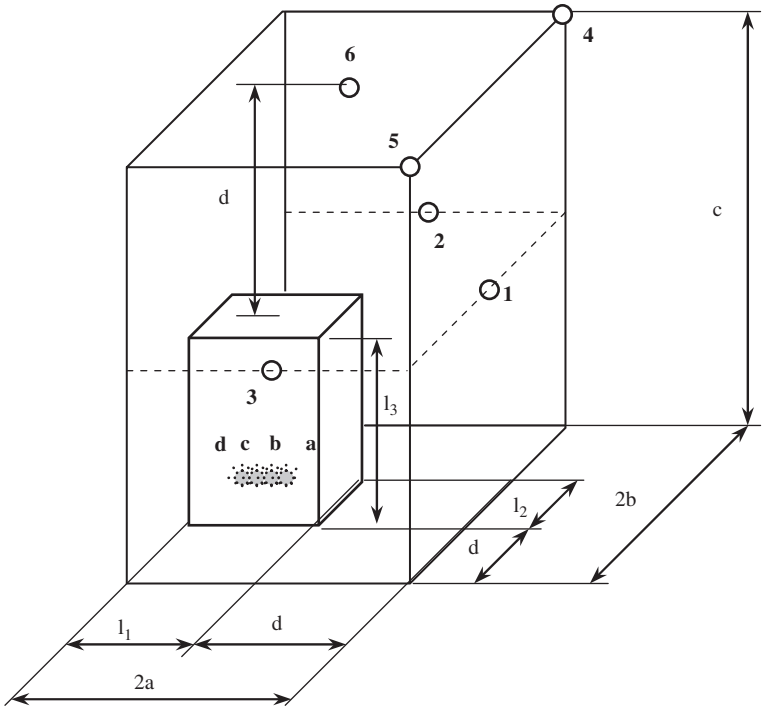

l_1=0.63m l_2=0.6m l_3=0.845m

a=0.815m b=1.3m c=1.845m

S=2 (2ac+2ab+bc) = 15.05m^2

Fig. 9. Measurement positions around the machine frame in semi-anechoic chamber according to ISO3741.

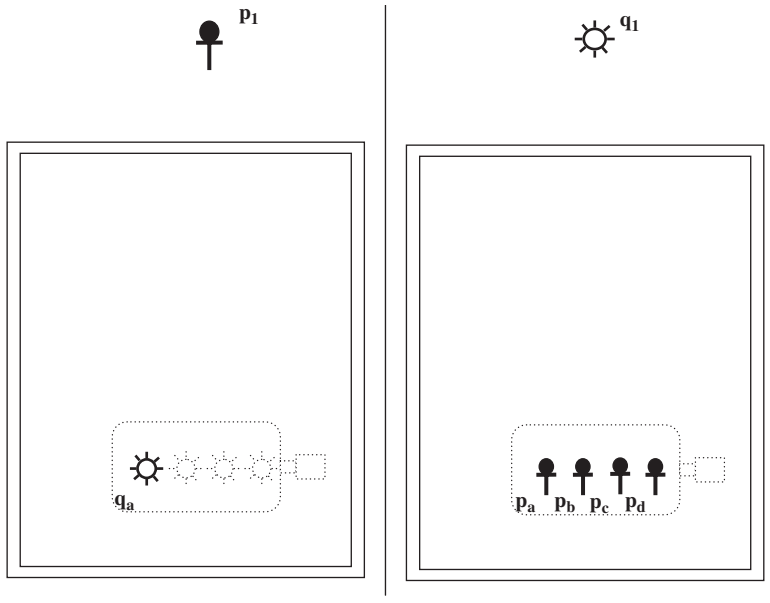

Fig. 10. Schematic of forward and reciprocal measurement set up for machine frame transfer function measurement.

4.1.1. Source

The source used for reciprocity measurements must be omnidirectional and of known volume velocity. In addition, there were particular requirements for this test: the measurement range was up to 10kHz, and a relatively high sound power was needed for measurement of structural transfer functions (which are reported in a later paper). The only source found to meet the power requirements was a dodecahedron loudspeaker. This met the requirements for omnidirectionality up to about 3kHz, but for higher frequencies it was necessary to rotate it on a rotating turntable (Fig. 11). The dodecahedron was calibrated by measuring its sound power. Two different methods were used so as to provide a cross check on the results. First, measurements were made with microphones located over a hemisphere in an anechoic chamber, and secondly the method of comparison with a reference source of known sound power in a reverberation room was used. The sound power obtained by both methods was found to be in good agreement, providing sufficient microphone positions were used in the anechoic chamber. Having obtained the sound power, the volume velocity of the dodecahedron was calculated using the well-known relationship for a monopole.

An electrical signal from the dodecahedron was initially used as a reference. However, poor coherence was obtained between the electrical signal and the microphones when the source was rotated. Consequently, microphone 'a' was used as a reference. The measured transfer functions therefore lack an absolute phase measurement, but the relative phase between all elements of the matrix is known. This is sufficient for prediction of output sound pressure magnitude and auralisation of steady-state signals which are the main requirements of a virtual acoustic prototype.

Fig. 11. Rotating dodecahedron loudspeaker use for reciprocal measurement of transfer functions.

4.1.2. Microphones

A cage in the form of a dummy motor (Fig. 12) was constructed allowing the microphones to be positioned precisely on the motor axis. The microphones can be placed, and repositioned to an accuracy of about 1 mm, which leads to good reproducibility. (Although it is not the main emphasis of this paper, it is practically important to obtain good reproducibility since small changes in frame performance, for example due to a design modification, can then be reliably measured. It is becoming increasingly important for machine manufacturers to be able to quantify such small changes as designs become more refined in terms of low noise, and the sub-structuring approach described here offers potential advantages in this respect over traditional 'forward' prototyping.)

4.2. Results and analysis of frame transfer functions

In total a 6×4 matrix of transfer functions was measured, a small sample of which are shown in Fig. 13. Also shown is the calculated result that would be obtained in free field; the difference between this and the measured curves is obviously related to the insertion loss of the frame.

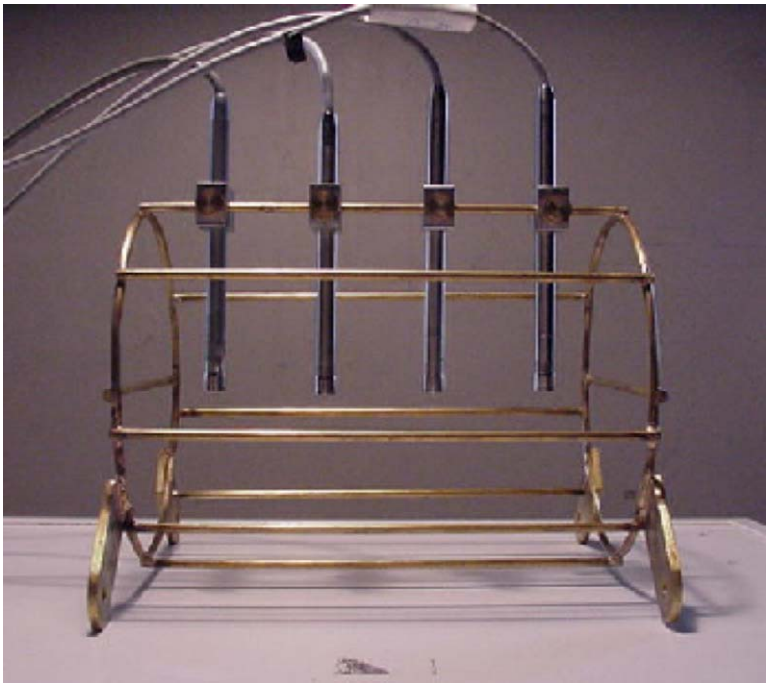

Fig. 12. Cage used to locate precisely the microphones on the motor centre line for reciprocal transfer of function measurement.

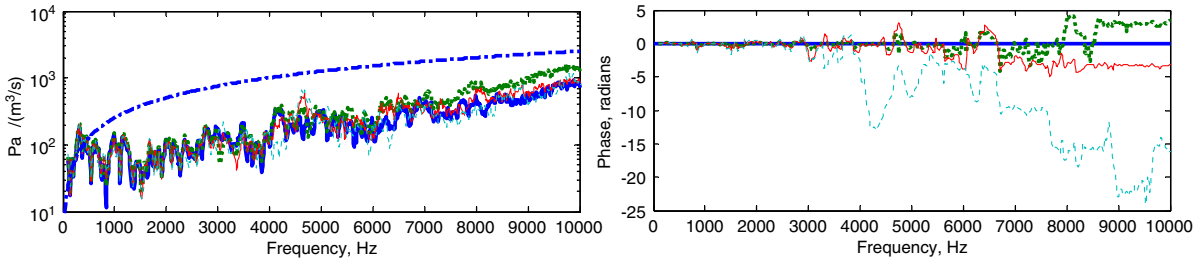

Fig. 13. Transfer function between external position 4 and internal positions. Upper: magnitude; ___, internal position a; ••••, b; ___, c; ...., d; - - - -, expected value without frame (free field). Lower: phase of position; ••••, b; ___, c; ...., d relative to position a.

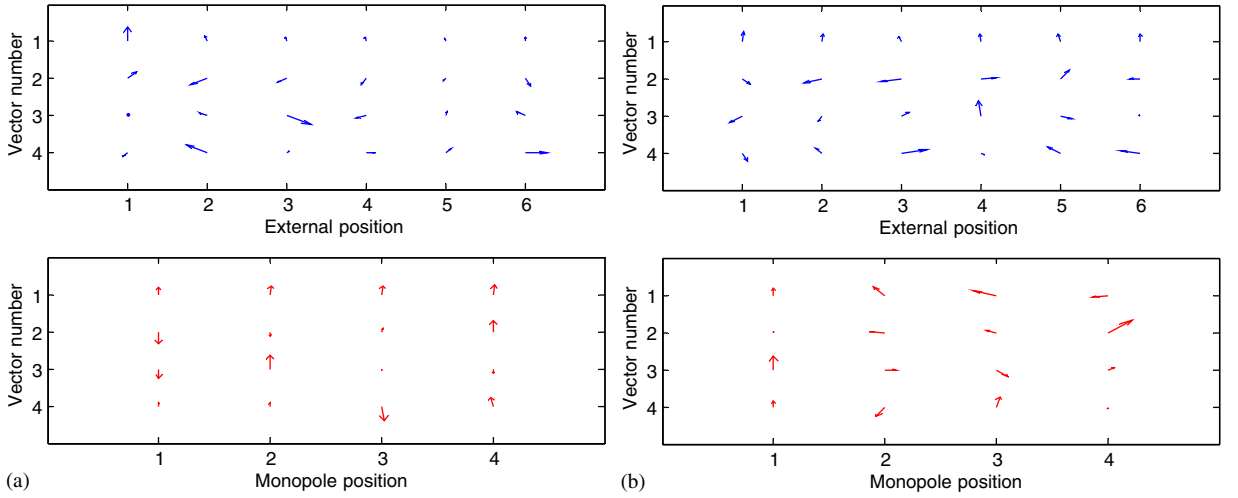

Fig. 14. Output (top) and input (bottom) singular vectors (input and output modes) from measured frame transfer function matrix at (a) 250 Hz and (b) 5000 Hz. The length of the arrow represents the magnitude of the (dimensionless) vector element, and the angle its phase.

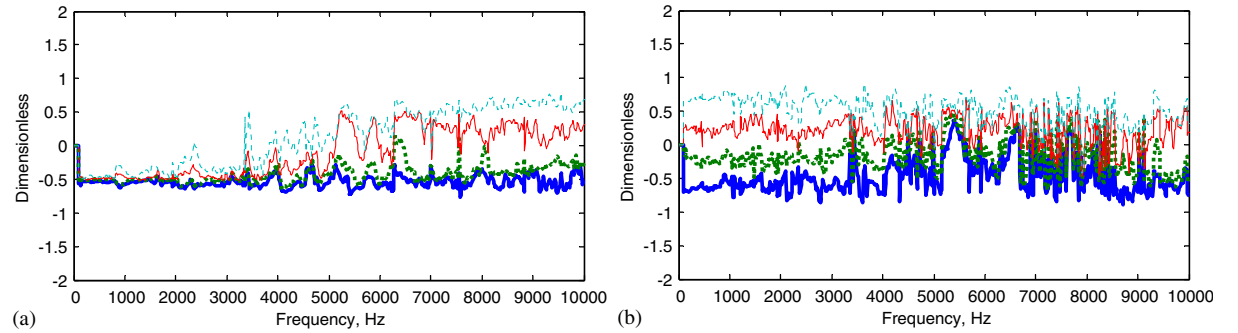

Fig. 15. Real parts of the input singular vectors (input modes) from the measured frame transfer function matrix corresponding to (a) the most efficiently radiating mode (dominant singular value), and (b) second most efficiently radiating mode: ___, monopole a; ••••, b; ___, c; . . . ., d.

It is instructive to carry out a singular value decomposition as was done for the motor in free field. Fig. 14(a) shows that at 250 Hz the input modes are similar to the free field case, even though the cavity is not symmetrical. The most efficiently radiating mode is with all four monopoles in phase and of equal magnitude. The second most efficient is the dipole type pattern. However, at 5000 Hz (Fig. 14b) the patterns are quite different from the free field case due to lack of symmetry inside the frame.

Fig. 15a plots the real part of the input singular vectors for the mode with the largest singular value as a function of frequency. It is seen that all terms are in phase and of comparable magnitude up to around 3kHz, i.e. an equivalent source acting as a single large monopole will radiate most efficiently. Fig. 15b shows that the second most important mode is a dipole type pattern, again up to 3kHz with sources a and d equal and opposite strengths, and b and c equal and opposite and of lower magnitude. These trends break down above 5kHz and more complicated behaviour takes over.

The singular values of the measured H are shown in Fig. 16, the free field counterpart of which was given in Fig. 5.

5. Prediction of sound output and validation

All the ingredients are now available to predict sound output from the assembled machine. Eq. (1) is used with **H**, the measured transfer function matrix. **q** is the vector of monopole source strengths obtained as a

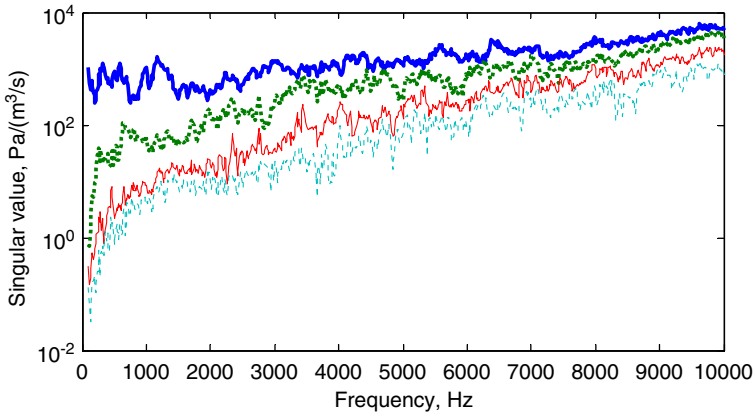

Fig. 16. Singular values from measured frame transfer function as a function of frequency for 12 mm spacing of the monopoles.

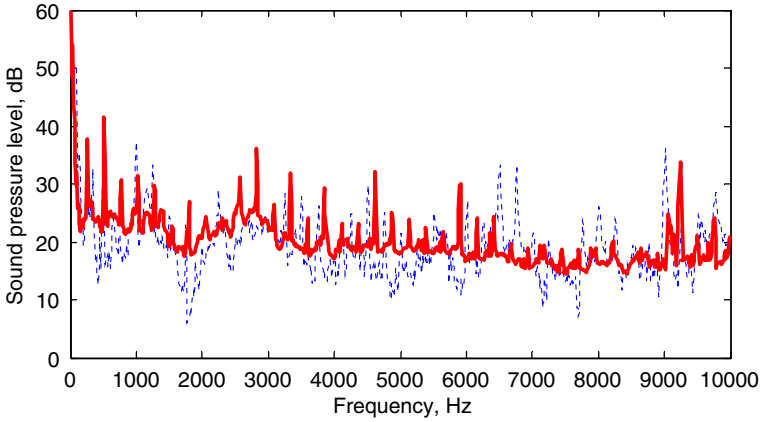

Fig. 17. Measured and predicted spatially averaged sound pressure level (dB re 20-μPa)l: ___, measured; ••••, predicted with three modes.

weighted sum of the selected input modes from Section 3: $\mathbf{q} = \mathbf{V_0 s_n} c$, where $\mathbf{s}_n$ is the source strength vector in the truncated modal basis, i.e. it is similar to $\mathbf{s}$ from Eq. (7), but with a reduced length corresponding to the retained (not discarded) singular modes, and c is a factor to compensate in magnitude for the discarded singular values as described in Ref. [23]. As mentioned above, the modes selected were zero and first order over the entire range, and second order from 5kHz upwards, so this will be termed a three-mode prediction.

To provide independent validation the motor was physically mounted inside the frame, but hung by string from its supports in order to eliminate structural transmission. Sound pressure was measured at the 6 external positions (Fig. 9). Fig. 17 shows a comparison of measured and calculated spatially averaged (rms average) sound pressure level in narrow band. The overall trend is reasonable although there are clear differences in detail. However, it was believed that the discrepancies were at least in part due to difficulties in running the motor at exactly the same speed for the 'free' and 'installed' motor tests.

Shown in Fig. 18 are the third octave results reconstructed from the narrow band results. Agreement is within 5 B for each band. The overall values were 51.1 dB measured and 51.1 dB predicted. Also shown on this plot is the predicted sound power obtained by discarding all modes except zero order. There is a discrepancy of 10 dB in the 800 Hz third octave, but elsewhere the agreement is as good as, or better, than for the three mode prediction. This is an interesting possibility, firstly because it suggests that the motor directivity is not needed, and secondly that fewer monopoles in the equivalent source, say two or even one, might suffice, thereby reducing the amount of data required. The relatively low influence of the directivity patterns around the motor can be explained by the fact that it was enclosed inside the machine cabinet. In theory, certain directivity patterns from the motor could couple more or less efficiently with some cavity modes, so directivity cannot be

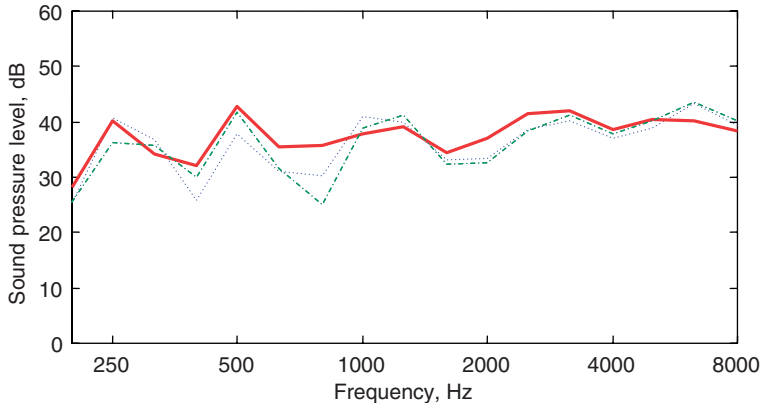

Fig. 18. Measured and predicted third octave band spatially averaged sound pressure level (dB re 20-μPa)l: ____, measured, predicted using source characterisation with: - - - -, three modes; –·–·–, one mode.

neglected a priori. However, the measured transfer functions shown in Fig. 13 do not indicate strong modal behaviour. This is to be expected given that the inside of the cabinet was lined with 15 mm of acoustically absorbing fibrous material, and that, due to a number of other components, the cavity space was complicated and irregularly shaped. Thus, we would expect some 'mixing' to occur in the cavity, so that the overall magnitude of the excitation appears to be more important than the spatial patterns. This is not necessarily a general result, although we might expect it to apply to other machine cabinets with a similar degree of geometric complication. Thus, although it might be possible to optimise the positions of the monopoles on the axis a more promising way forward, in line with the objectives, was to simplify the representation as much as possible, which will be considered in the next section.

5.1. Prediction using a single monopole

In the light of the above results it was decided to attempt to characterise the motor by a single monopole at its centre. This allows a considerable simplification in the test procedure since the sound power of the motor is sufficient to calculate the single monopole strength. Therefore, any measure of sound power could be used. A reverberation room method was used (ISO3741, 2000) with a single microphone on a rotating boom, and the volume velocity of the equivalent source was calculated according to the well-known relationship for a monopole:

$$W = (\rho_0 \omega^2 / 8\pi c_0)|q_m|^2 \tag{9}$$

in which W is the measured sound power freely suspended motor, and q_m is the volume velocity of the equivalent monopole, ρ_0 and c_0 are the density and speed of sound in air, and ω the radian frequency.

An improved motor controller was obtained which allowed the speed to be kept constant within about 2% for the duration of the two minute measurement. Measurements were repeated at four running speeds, 7436, 12690, 14350, 16220 rev/min. Measurements of installed sound power were conducted in the same way, but with the motor installed inside the machine cabinet.

Transfer functions were also obtained in a reverberation room using a reciprocal technique as described above. The transfer functions therefore include not only the effect of the frame as before, but also the effect of room reverberance. In initial tests, a single microphone was used at the centre of the motor for the reciprocal tests. However, it was subsequently found that better results were obtained by taking an rms average of the results from four microphones spaced apart by 12 mm along the motor axis, using an arrangement similar to that in Fig. 12.

The sound power calculated from the virtual prototype approach is compared with the directly measured sound power in Figs. 19 and 20. Four speeds were tested for two different motors, the results in Fig. 19 are among the best and Fig. 20 among the least good results. The peaks in the narrow band plots have been

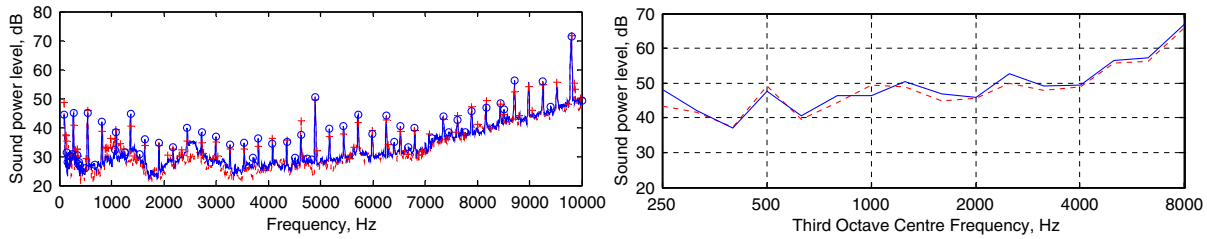

Fig. 19. Measured and predicted sound power level (dB re 1-pW) using a single monopole equivalent source for motor speed of 16 200 rev/min. Upper, narrow band; lower, third octave bands.

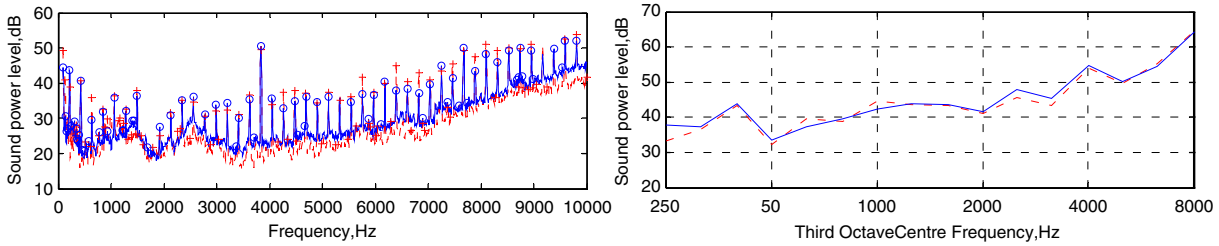

Fig. 20. Measured and predicted sound power level (dB re 1-pW) using a single monopole equivalent source for motor speed of 12700 rev/min. Upper, narrow band; lower, third octave bands.

highlighted with symbols to aid comparison, and it is seen that good agreement is obtained at nearly every peak. Furthermore, the broadband 'baseline' agrees well. Third octave band plots are given in the lower half of Figs. 19 and 20 and show good agreement with nearly every band within 2 dB of the measured values. The overall linear dB and dBA values (not shown) agreed to within 0.1 dB.

The results from this section indicate that the results from the single monopole representation are considerably better than those for the multiple monopole. This does not necessarily imply that the single monopole is a superior source characterisation in terms of accuracy. There are two main reasons. Firstly, better motor control meant that the same operating conditions were obtained for the virtual and the real prototypes. Secondly, it is thought that the method of measuring transfer functions in a reverberation room as opposed to an anechoic chamber is probably more accurate. In the latter method, spatial averaging was achieved by averaging over six external positions. However, it was experienced during testing that the measured transfer functions were sensitive to the position of the external points, particularly at high frequencies. In the reverberation room, spatial averaging is achieved by multiple reflections from the walls, equivalent to many more than six positions, such that the averaging is more robust. Thus, although the single monopole is not a 'more accurate' source characterisation per se, its simplicity allows simpler and more robust measurements to be used to obtain the required source characterisation data. Ultimately, it is considered that the greater robustness of the measurements is more likely to lead to a good prediction than a more complicated and delicate procedure, particularly since the procedure is to be applied as a working method for medium technology industries.

6. Concluding remarks

A general scheme for producing virtual acoustic prototypes has been described and illustrated by an example of a real machine. In the scheme, the machine is separated into two substructures, the 'component', and the 'frame'. Both substructures are characterised by measured data, obtained independently of the assembly. The data is then combined so as to represent the overall sound output of the assembled machine. The 'assembly' is a simple type of virtual acoustic prototype, in which active components can be substituted in the virtual domain without the need to assemble a physical prototype for each.

The general methodology is to characterise the source by considering it as an equivalent source system made up of a combination of elementary sources. The equivalent source system for the motor consisted of a number of monopoles located along the axis of the motor. Their (complex) source strengths were determined by an inverse method from the measured free field sound pressure around the motor. Initially, four monopoles were used, and this was subsequently simplified to a single monopole.

Comparison of the real and virtual prototype showed reasonable agreement for the four monopole model. This was limited, at least in part, by the fact that the motor running condition could not be exactly repeated. Comparison for the single monopole (using an improved motor controller) was excellent. It appears that, in practice, the simpler equivalent source works better because the measurements to obtain the source and frame data can be conducted in a reverberation room, in which the spatial averaging of sound pressure is more effective than can be obtained in anechoic conditions.

It might be thought that a limitation of the approach is that the transfer functions for the frame must be re-measured after design modifications. However, there is no theoretical reason why numerically calculated transfer functions cannot be used in place of measured ones. An example is given in Ref. [27], in which measured source data was combined with transfer functions obtained from boundary element methods. As it stands the approach is well adapted to designers who lack the resources to construct large-scale numerical models, but need a more cost-effective alternative than physical prototypes to compare the installed performance of active components like motors.

Acknowledgements

This work was partly carried out within EC funded project NABUCCO (GRD–1999-10785). Funding by the European Commission is gratefully acknowledged.

References

[1] A.T. Moorhouse, G. Pavic, Virtual acoustic prototypes of white goods products, *Proceedings of Inter-noise 2004*, Prague, Czech Republic, 2004.
[2] A.T. Moorhouse, Use of a hybrid measured-calculated mobility matrix for simplified calculation of structure-borne sound from an electric motor, *Proceedings of the 10th International Congress on Sound and Vibration*, Stockholm, 2003.
[3] L. Cremer, Die Synthese des Schallfeldes eines beliebigen festen Koerpers in Luft mit beliebiger Schnelleverteilung aus Keguelschallfeldern, *Acustica* 55 (1984) 44.
[4] M. Ochmann, The source simulation technique for acoustic radiation problems, *Acustica* 81 (1995) 512–527.
[5] Y.I. Bobrovnitskii, T.M. Tomilina, Calculation of radiation from finite elastic bodies by the method of auxilliary sources, *Soviet Physics Acoustics* 36 (4) (1990) 334–338.
[6] G.H. Koopmann, L. Song, J.B. Fahnline, A method for computing acoustic fields based on the principle of wave superposition, *Journal of the Acoustic Society of America* 86 (6) (1989) 2433–2438.
[7] Y.I. Bobrovnitskii, T.M. Tomilina, General properties and fundamental errors of the method of equivalent sources, *Acoustical Physics* 41 (5) (1995) 649–660.
[8] L. Bouchet, T. Loyau, N. Hamzaoui, C. Boisson, Calculation of acoustic radiation using equivalent-sphere methods, *Journal of the Acoustic Society of America* 107 (5) (2000) 2387–2397.
[9] J.H. Zheng, F.J. Fahy, D. Anderton, Application of a vibroacoustic reciprocity technique to the prediction of sound radiated by a motored IC engine, *Applied Acoustics* 42 (4) (1994) 333–346.
[10] J.W. Verheij, Inverse and reciprocal methods for machinery noise source characterisation and sound path quantification—part 1: sources, *International Journal of Acoustics and Vibration* 2 (1997) 11–20.
[11] N. Attalla, G. Winckelmans, F. Sgard, A multiple multipole expansion approach for predicting the sound power of vibrating structures, *Acustica* 85 (1999) 47–53.
[12] Y.I. Bobrovnitskii, K.I. Mal'tsev, N.M. Ostapishin, S.N. Panov, Acoustical model of a machine, *Soviet Physics Acoustics* 37 (6) (1991) 570–574.
[13] M. Heckl, Bemerkung zur Berechnung der Schallabstrahlung nach der Methode der Kugelfeldsynthese, *Acustica* 68 (1989) 251–257.
[14] Y.I. Bobrovnitskii, T.M. Tomilina, Calculation of radiation from finite elastic bodies by the method of auxiliary sources, *Soviet Physics Acoustics* 36 (4) (1990) 334–338.
[15] E.G. Williams, J.D. Maynard, E. Skudrzyk, Sound source reconstructions using a microphone array, *Journal of the Acoustic Society of America* 68 (1) (1980) 340–344.
[16] H. Boden, The multiple load method for measuring the source characteristics of time-variant sources, *Journal of Sound and Vibration* 148 (3) (1991) 437–453.

[17] Y.I. Bobrovnitskii, G. Pavic, Modelling and characterisation of airborne noise sources, *Journal of Sound and Vibration* 261 (2003) 527–555.
[18] A.T. Moorhouse, Acoustic design by listening: techniques for simulating the sounds of machines and products, *Proceedings of NOVEM* 2005, St. Raphael, France, 2005.
[19] A.T. Moorhouse, R.D. Cookson, G. Seiffert, Measurement of operating forces of an electric motor, *Proceedings of NOISE-CON 2004*, Baltimore, USA, July 2004.
[20] P.A. Nelson, S.H. Yoon, Estimation of acoustic source strength by inverse methods—part 1: conditioning of the inverse problem, *Journal of Sound and Vibration* 233 (4) (2000) 643–668.
[21] P.A. Nelson, S.H. Yoon, Estimation of acoustic source strength by inverse methods—part 2: experimental investigation of methods for choosing regularization parameters, *Journal of Sound and Vibration* 233 (4) (2000) 669–705.
[22] E.G. Williams, Regularization methods for near-field acoustical holography, *Journal of the Acoustic Society of America* 110 (4) (2001) 1976–1988.
[23] A.T. Moorhouse, Compensation for discarded singular values in vibro-acoustic inverse methods, *Journal of Sound and Vibration* 267 (2) (2003) 245–252.
[24] T.M. Tomilina, Y.I. Bobrovnitskii, V.B. Yashkin, A.A. Kochkin, Power output of noise sources operating near elastic scatterers of finite dimensions, *Journal of Sound and Vibration* 226 (2) (1999) 285–304.
[25] BS EN ISO 3744:1995, Acoustics. Determination of sound power levels of noise sources using sound pressure, Engineering method in an essentially free field over a reflecting plane, 1995.
[26] F.J. Fahy, The vibro-acoustic reciprocity principle and applications to noise control, *Acustica* 81 (6) (1995) 544–558.
[27] A. Moorhouse, P.-O. Berglund, F. Fournier, T. Avikainen, Fan characterisation techniques, *Proceedings of Fan Noise 2003*, Senlis, France, 2003.